*Faraday Discuss.*, 1991, **92**, 1-11



# Introductory Lecture

# Blazing the Trail from Metals to Nuclei

**A. Howie**

*Cavendish Laboratory, University of Cambridge, Madingley Road, Cambridge CB3 0HE, UK*

Emphasis is given to studies of individual clusters. Molecular beam experiments indicate that in isolated metal clusters the stability, shape and several other properties are often dominated by electronic rather than atomic packing effects. Magic numbers arise as in nuclear shell theory. Electron microscopy of supported clusters indicates a preference for simple crystal including icosahedral, though often imperfect, structures and the smallest clusters can be unstable under electron illumination. The possibility of reconciling these results is discussed.

Major operations of chemical industry, substantial parts of materials technology and exciting new developments in medicine, depend on the properties of the ultrafine metal particles which Faraday[1] brought to scientific attention. In practical significance this late work may thus come to rival even Faraday's earlier achievements in electromagnetism, but so far the cluster scientist has nothing in terms of basic understanding which can be compared in power and completeness with Maxwell's theory. A crucial obstacle here has been the lack of samples with the kind of monodispersion of identical objects which have provided a basis for molecular chemistry and biology as well as for atomic and nuclear physics. In making a selection from the impossibly long list of topics which might be included in this introduction to the discussion, I have therefore chosen to emphasise two approaches which measure the properties of individual particles. Although such a line of attack may seem to take us away from the world of useful applications, it is the bias of a physicist to believe that it will pay dividends in the long run.

Faraday's term 'finely divided metal' still has both practical and conceptual relevance. Clusters may usually grow from smaller to larger by coalescence or by atomic addition but fragmentation processes are also used both in molecular beam experiments and in catalyst regeneration. As a convenient definition of what we mean by a metal particle, the reference to bulk properties avoids the serious demarcation problems caused by the operation of metal-insulator transitions (in either direction) as a function of particle size. On the intellectual trail which connects metals, clusters and atoms, the bulk metal retains a unique status as a fixed point but many of the recent cluster beam results now point beyond the atom to the atomic nucleus as our more logical ultimate destination.

## Properties of Isolated Clusters

A considerable number of measurements has now been reported and reviewed[2-6] of isolated clusters, formed with supersonic nozzle or gas aggregation sources in molecular beam equipment. Mass abundance spectra of neutral alkali metal (Na, K and Cs)

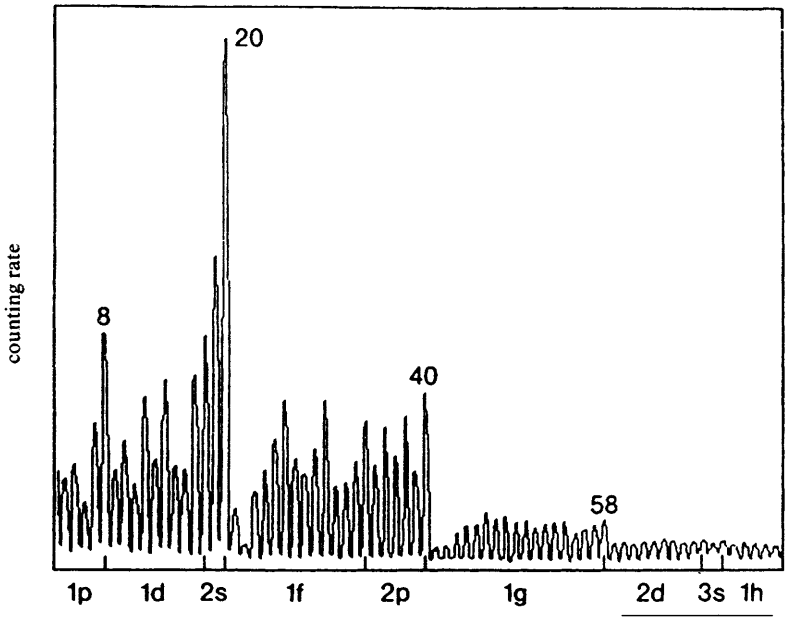


**Fig. 1** Mass abundance spectrum of sodium clusters showing shell structure due to electronic effects[77]

clusters obtained by time of flight methods show pronounced features (usually a rise to a maximum followed by an abrupt drop) at magic numbers of 8, 20, 40, 58, 92 .... An example is shown in Fig. 1. Similar effects in the abundance spectra of ionised clusters show that the magic numbers are definitely associated with the total number $n$ of valence electrons in the cluster and not with the number of atoms. Full interpretation of these results is obviously dependent on assumptions about the kinetic or thermodynamic conditions which apply in the production process. Variations of the pressure and temperature conditions in the source change somewhat the detailed shape of the abundance peaks but not, however, their positions, *i.e.* the magic numbers are unaffected. For $Cu^+$, $Ag^+$ and $Au^+$ clusters[6] the same magic numbers have been found for total valence electron numbers in the cluster. Ionisation potentials, measured by extrapolation from photo-ionisation efficiency spectra, show similar peaks when the total number $n$ of valence electrons in the cluster corresponds to a magic number with a sharp drop on the high side of the peak. Taken together these experiments demonstrate rather convincingly that there is a strong electronic effect which controls cluster stability with peaks in stability, *i.e.* energy minima, occurring when the total number of valence electrons coincides with one of the magic numbers. Below $n = 40$ an odd–even oscillation in the abundance spectra is often also seen, suggesting that electron-pairing plays some role in stability in this regime. These magic numbers are clearly quite different from the ones that might be expected for the number of atoms in regular polyhedra such as cubo-octahedra or icosahedra (13, 55, 147, 309, 561, 923 ...) and which have indeed been found[4,7] and verified by electron diffraction[8] for clusters of Xe and other rare gases.

The coincidence of the magic numbers for electrons in clusters with those familiar for electrons in atoms and for nucleons in nuclei strongly suggests that they are caused by similar shell structure effects in the filling of energy levels. Indeed, a surprisingly good, semiquantitative explanation of the results is given by the crudest jellium model where the $n$ valence electrons are delocalised and move independently in a spherically

symmetric square-well potential whose radius is fixed by the measured bulk density. Each energy level is described with quantum numbers $n_r$ and $l$ (giving the number of radial and angular nodes respectively) and (including spin) is $2(2l+1)$ fold degenerate. Such a potential is much more similar to the nuclear potential than to the screened Coulomb potential in the atom, the atomic restriction $l \leqslant n_r$ does not apply and the energy depends roughly on $3n_r + l$. In atoms, shell structure is observed for $l \leqslant 3$ and in nuclei for $l \leqslant 6$. Recent observations of mass-abundance spectra with large Na clusters[9] as well as $Cs_{n+2z}O_z$ and $Cs_{n+2}(SO_2)$ clusters,[10] all with $n$ delocalised electrons, have demonstrated shell structure for $l \leqslant 12$ with magic numbers at 2, 8, 20, 40, 58, 92, 138, 196, 260, 344, 440 and 558. Electronic shell structure effects have also been reported[11] in the mass spectra of Na clusters up to $n = 1500$ with further structure up to $n = 22\,000$ however being ascribed[11,5] to the formation of either cubo-octahedral or icosahedral atomic structures.

The strong evidence that the behaviour of valence electrons in clusters can mimic and even extend the known results for shell structure in nuclei is an astounding result. It seems likely that the analogy will also include the ellipsoidal distortions which are well studied in nuclei and which occur when angular momentum shells are only partially filled so that spherical symmetry is lost. Photo-absorption experiments[12] indeed already indicate a splitting of the surface plasmon resonance for Na clusters lying between magic number values which may well be due to such a Jahn–Teller distortion to a spheroidal shape. The jellium model can be substantially improved with the incorporation of a more self-consistent potential derived from the electron density. This potential is no longer flat-bottomed but has a weak maximum at the origin and a smoother outer limit corresponding to the spill-over of electron charge at the cluster surface. The modified charge distribution both inside and outside the cluster results in a significantly better fit to measured polarisability and other excitation properties.[2]

Because of the closed s shell in the atom, divalent element clusters display more complex behaviour, with shell structure reported[2] for Cd and Zn but a transition from van der Waals through covalent to metallic binding occurring in Ba and Hg for 30–60 atom clusters.[13,14] In Mg, icosahedral packing effects are reported[15,5] in the mass spectra of clusters with 147–2869 atoms but electronic structure effects are dominant for smaller clusters. Deviations from the simple electronic shell structure predictions are also observed[16] in Al where full s–p hybridisation occurs only in larger clusters. A peak in ionisation potential for the 13-atom cluster for instance is identified[16] with an icosahedral structure. For isolated transition-metal clusters the results are so far much harder to interpret[17] at least on the jellium model because of the localised nature of the d electrons. Nevertheless, the ability of small Pd clusters to bind hydrogen[18] and react with various other gases[19] varies strongly with cluster size and can attain remarkably high values of 3–8 molecules per cluster atom. The steady evolution of the d-band structure, developing for just a few atoms and reaching effectively the bulk form for more than 100 atoms, has been investigated in mass selected Cu clusters[20] and in Ag and Pd clusters[21] by UV photoelectron spectroscopy.

## Structural Computations for Isolated Clusters

Because of the regrettable absence of direct structural observations, computations have come to play an increasingly important part in cluster physics, including indeed an independent prediction[22] of shell structure effects. There are two serious difficulties to be overcome; firstly the calculation of adequate many electron wavefunctions and energy levels for any given atomic arrangement and secondly the search for the optimal atomic arrangement corresponding to an absolute minimum in a total energy surface which is inevitably very complex with a large number of secondary minima. Even with present day computers, the approach to wavefunction computation *via* the Hartree–Fock

method (including configuration interaction to deal with electron correlation effects) is impractical for the cluster sizes of interest. The approach which is increasingly widely used in solid-state physics as well as some molecular problems is the density-functional formalism in which wavefunctions are computed for independent electrons moving in a potential which is determined self-consistently from the total ion and electron density but also includes a contribution which approximates the effects of correlation and depends on the local electron density. Clearly such a model cannot be expected to cover strong correlation effects completely and other compromises have been suggested.[23] A critical review has been given[24] of the density-functional technique and of its striking successes in predicting the ground-state energies of a wide variety of systems. An important advance occurred when Car and Parrinello[25] showed how the density-functional technique could be combined with molecular dynamics, simulated annealing methods resulting in an efficient search procedure for the lowest energy configuration for both electrons and ions in, for example, a cluster. Applications of the Car–Parrinello method to cluster computations are surveyed[3] for Na (where planar structures for smaller clusters give way to more spherical forms for larger clusters[26]). A similar trend is noted in computations[27] for Al clusters which show a variety of structures of closely similar energy with icosahedral structures arising for 13-atom and 55-atom clusters (see accompanying paper[28]). Substantial effort has also been put into the computation of Si clusters.[29,30] In agreement with experimental observations, stable magic number clusters are found for $Si_{33}$ and $Si_{45}$ which are chemically inert because the surface has reconstructed to remove dangling bonds. The interior of these clusters seems still to be tetrahedrally bonded however so no great violence will be done if they are ruled out from the present discussion according to Faraday's definition of metal clusters.

## Structure of Individual Supported Particles

Electron microscopy in a variety of imaging modes has in recent years come to play an increasingly important role in catalyst characterisation[31,32,33] and together with other techniques is addressing more precisely some of the long-standing questions[34] over the role of small metal particles in heterogeneous catalysts. For the study of more detailed structure in individual supported particles, particularly in the size range above 2 nm, high-resolution transmission electron microscopy is now recognised as an exceptionally powerful procedure. The bright field images generally employed are formed by a coherent, phase contrast process and the images are essentially two-dimensional projections with enough resolution to resolve individual planes or columns of atoms in a well oriented crystalline particle. In many cases useful information about the size, shape and structure of an individual particle is quickly available. The images can also be quantitatively compared with theoretical simulations to confirm in more detail the validity of any assumed structure or the thickness of the particle in the beam direction, see for example accompanying paper[35] and ref. 36. In many cases, bulk single crystal structures are observed with simple polyhedral shapes (cubes, cubo-octahedra *etc.*). In other cases of normally f.c.c. metals particularly Au, Ag but much more rarely Pt or Pd, twin defects are observed in the particles. These can take the form of single twins or lamellar twins lying parallel to one another. More spectacularly however, more symmetrical, multiply twinned particles (MTP) are found as decahedra or icosahedra consisting respectively of 5 and 20 tetrahedral units joined internally in twin relation across (111) faces and presenting their other (111) low surface energy faces to the outside of the particle (for images and references see accompanying paper[35]). Below a certain particle size, estimated[37,38] from bulk metal parameters to be *ca.* 10 nm in Au, the MTP are energetically preferred to single-crystal polyhedra since they have reduced surface energy at the cost of some internal twin boundary and elastic strain energy. One often observes MTP much larger than this critical size, possibly because a growing particle which adopts

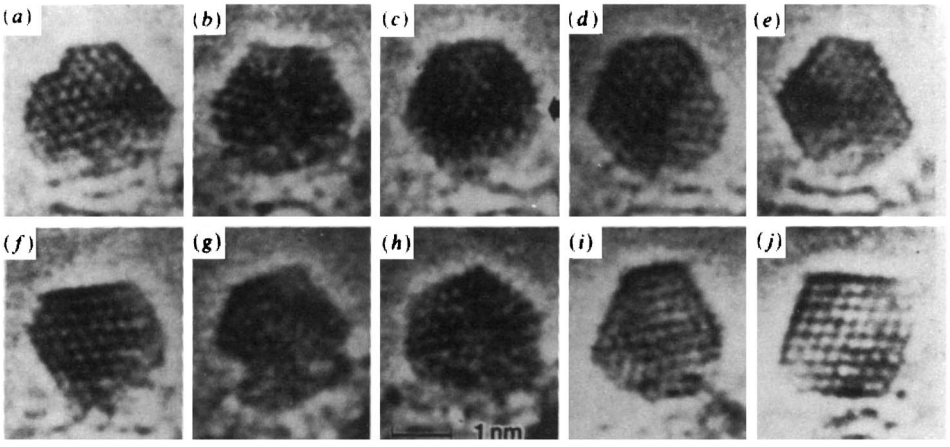


**Fig. 2** Sequence of structures adopted by a 2 nm Au particle observed[46] by high resolution electron microscopy

this structure at an early stage may find it difficult to revert to the single-crystal form, even if this has lower energy. Large MTP may be stabilised by the presence of additional chemical ligands as well as by the dislocations which they are sometimes observed[38] to contain and which serve to lower the internal strain energy. MTP have been found[39] in working catalysts and Au colloids[40] prepared according to Faraday's procedures contain micro-twinned particles, but so far there is no unequivocal demonstration that these structures have, *via* their surface facets, any specific catalytic or other chemical significance of the type so thoroughly explored in bulk single-crystal studies.[41]

The surface structure of small particles can often be studied in profile images[42,43] which are obtained when a surface facet is aligned parallel to the beam direction. These profile images show surface step structures and surface reconstructions[42,44], some of which are identical with the reconstructions found on bulk single-crystal surfaces. Twin boundary grooving effects consistent with surface energy minimisation[37] are also evident in some MTP, particularly decahedra.

Under the influence of the electron beam, dynamic events are sometimes observed, including not only motion of surface steps on particles but also, in the case of particles of size less than *ca.* 2 nm, dramatic changes of internal structure. Video sequences[45,46] show abrupt changes of structure from MTP structure to single crystal, to amorphous or possibly molten structure on a typical time scale of *ca.* 1 s. An example is shown in Fig. 2. It has been argued[47,48] that this phenomenon is unlikely to be a purely thermal effect, but may be explained by comparatively rare events in which the particle receives unusually large transfers of energy, momentum or charge from the electron beam, causing it to flip between structures of rather similar energy.

The conventional methods of high resolution transmission microscopy are less successful for particle sizes below *ca.* 1 nm because it becomes difficult to distinguish the particle from the background image noise generated by the often rather random structure of the support. In the most usual case of heavy atom clusters on a light atom support, the scanning transmission electron microscope (STEM) offers a solution to this problem since dark field, Z-contrast images can be formed using electrons which have been scattered through appreciable angles in close encounters with high atomic number atoms.[49,50] In the high-resolution STEM very small heavy-atom clusters,[51] containing as few as three atoms,[52] can then be detected as bright images against the background intensity from a typical 20 nm support film. The size of the small cluster can be estimated

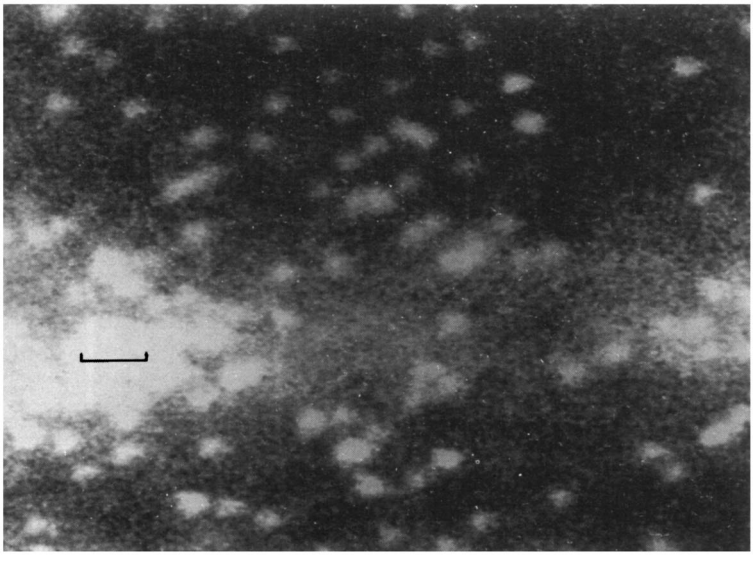

**Fig. 3** Annular dark field Z contrast STEM images obtained[53] from $Os_{20}(CO)_{40}$ clusters dispersed on a carbon film. The scale bar denotes 3 nm

from the integrated intensity in the image.[52] Recently it has proved possible[53] to image $[Os_{20}(CO)_{40}]$ clusters on a carbon support film where, as shown in Fig. 3, the expected triangular shape of the clusters is just discernible. These organo-metallic clusters were kindly made available to us by Prof. Lord Lewis and his colleagues (for further references see accompanying paper[54]). The presence of many other features in Fig. 3 suggests that many of the clusters may have agglomerated in the deposition stage. They do however appear to be stable under the electron beam. More generally, STEM images of very small clusters sometimes exhibit changes between successive scans indicating the occurrence of dynamic events. These are no doubt frequently induced by the electron beam irradiation but, as has been convincingly shown by Crewe,[55] may also be due to simple thermal effects independent of the beam.

Although it provides only statistical information rather than information about individual particles, the EXAFS method is potentially a powerful complement to high-resolution electron microscopy, particularly for particles in the difficult by significant size range below 1 nm. A rather thorough survey of the large number of heterogeneous catalyst systems which have been studied has recently been published[56] and includes bimetallic systems as well as cases where the metal seems to be partially dispersed as single atoms in the support. So far there have been no cases where MTP structures have been detected by EXAFS, possibly because most of the work has been on Pt and Pd clusters where these structures do not frequently occur. It would certainly be interesting to obtain EXAFS data from a system which is known to contain a high fraction of MTP. This would be a useful test of the sensitivity of the method and might also provide valuable data about the inhomogeneous internal elastic strain in MTP.

## Electron Spectroscopy of Individual Particles

In addition to the Z-contrast imaging technique just described, there are several other facilities available in the STEM which yield valuable information about individual small

particles.[31] These include microdiffraction,[57] X-ray nanoanalysis in bimetallic Pt–Rh particles,[58] secondary electron imaging[59] and Auger spectroscopy[60] with 3 nm spatial resolution. Energy loss spectroscopy of the primary electron beam can achieve better than 1 nm spatial resolution and an energy resolution of 1 eV and can now be carried out with great efficiency, thanks to the development of parallel detection systems[61,62] which allow the whole spectrum to be collected simultaneously.

In the higher part of the loss spectrum between *ca.* 80 eV and 2 keV, characteristic edges from inner-shell excitations are observed. These are mainly employed as a means of nanoanalysis which has already proved its value in a variety of cluster and interface studies.[63,64] These characteristic edges also display chemical shifts and shape changes such as white lines as well as oscillatory features similar to EXAFS effects above the edge. Although some pioneering studies have made use of these phenomena, they have largely untapped potential in small particle studies.

Information about valence electron excitations is contained in the relatively intense, low loss part of the spectrum below 50 eV. As first shown by Fermi[65] for a homogeneous medium, the intensity at energy loss $\Delta E = \hbar\omega$ in the loss spectrum is described by a characteristic bulk loss function.

$$\mathrm{Im}\,[-1/\varepsilon(\omega)] = \varepsilon_2(\omega)/(\varepsilon_1^2+\varepsilon_2^2) \tag{1}$$

where $\varepsilon(\omega) = \varepsilon_1(\omega)+\mathrm{i}\varepsilon_2(\omega)$ is the frequency-dependent, complex dielectric function of the material. More generally $\varepsilon$ will depend on momentum transfer as well as energy transfer. The real and imaginary parts of $\varepsilon$ are not independent and a determination of $\varepsilon_2(\omega)$ (which is related to optical absorption) can be used to find $\varepsilon_1(\omega)$. Eqn. (1) shows that in regions where $\varepsilon_1$ is not too small, the electron energy loss spectrum can show peaks related to the peaks in optical absorption and associated with single electron transitions. Generally more prominent however are the collective loss peaks or plasmons which arise when $\varepsilon_1(\omega) = 0$ and $\varepsilon_2(\omega)$ is small.

In the last few years, Fermi's theory has been greatly extended (for references see ref. 66 and 67) to deal with the inhomogeneous situations of interest in electron microscopy. For instance, near a planar interface between two media A and B, a characteristic loss function $\mathrm{Im}\,\{-1/[\varepsilon_A(\omega)+\varepsilon_B(\omega)]\}$ is observed which can give rise to interface or (in the case of a vacuum interface) surface plasmons. Fast electrons of velocity $v$ travelling parallel to the interface, and within a typical distance $v/\omega$ of it, generate these interface losses rather than bulk losses. Excitations on spherical particles have also been extensively studied. In general both bulk and surface losses corresponding to different angular quantum numbers $l$ are observed. For very small spheres of material A with radius $a < v/\omega$ embedded in another material B, the surface $l = 1$ dipole loss dominates and is described by the function $\mathrm{Im}\,[-1/(\varepsilon_A+2\varepsilon_B)]$. Walls and Howie[67] showed that with systematic application of these methods a complete and self-consistent dielectric characterisation of an individual small particle can be achieved. The method is also capable of detecting the presence of adsorbed or modified surface layers on such a particle.[68] In future work it will be important to take better account of the influence of the support and some progress has been made with this.[69]

Given the interest in colloids at this Discussion, it may be useful to draw attention to a recent extension of the dielectric excitation theory to the case where a large number of particles are present in the irradiated region and cannot be resolved individually in the image. For such cases, Howie and Walsh[70] have proposed an effective loss function given by the expression

$$\frac{1}{\varepsilon_{\mathrm{eff}}} = f\left[\frac{1}{\varepsilon_A}+g_{\mathrm{int}}\left(\frac{3}{\varepsilon_A+2\varepsilon_B}-\frac{1}{\varepsilon_A}\right)\right]+(1-f)\left[\frac{1}{\varepsilon_B}+g_{\mathrm{ext}}\left(\frac{3}{\varepsilon_A+2\varepsilon_B}-\frac{1}{\varepsilon_B}\right)\right] \tag{2}$$

where $f$ is the volume fraction of material A. The first term multiplied by $f$ describes the fraction of the fast electron trajectories which are inside the small particle and able to generate either bulk or (in regions close to the particle surface) dipole interface losses. Based on the work with isolated spheres[71] a suitable form for the function $g_{int}$ might be

$$g_{int} = \frac{1}{1+3a\omega/v} \tag{3}$$

The second major term in eqn. (2) describes the contribution from segments of trajectories outside the particles and once again exhibits both bulk and surface losses. For small values of $f$ we might expect $g_{ext}$ (which measures the fraction of external volume close to a particle surface) to be proportional to $f$. An interesting point about eqn. (2) is that in the limit of very small spheres, where $g_{int} = 1$ and there is no bulk contribution from material A, the equation is completely equivalent to the well known Maxwell Garnett[72] effective medium theory, provided we take $g_{ext} = 2f/(1+2f)$. The Maxwell Garnett (MG) theory has been used with some success to interpret the optical properties of colloids; however, as found by Howie and Walsh,[70] it is much less successful than eqn. (2) in fitting the observed electron loss spectra from small particles of Al in a colloidal dispersion. These observed spectra are shown in Fig. 4($a$) and exhibit an interface loss at 6–8 eV and an Al bulk plasmon loss at 15 eV which build up progressively as the colloid grows (as a result of electron beam damage). There is a related decay of the 25 eV loss from the surrounding $AlF_3$ matrix which decomposes during the process. The loss functions computed from eqn. (2) are shown in Fig. 4($b$) and qualitatively reproduce the main features of the observed spectrum. The MG theory gives an interface loss but no bulk Al loss. Angle-resolved energy loss experiments[73] on K clusters embedded in MgO thin films display in more detail the momentum dependence of the suppression of the bulk plasmon with decreasing cluster size.

## Discussion

There is so far complementarity and only a very small degree of overlap between the molecular beam results or computations for isolated clusters and the electron microscopy observations of supported clusters. The tendency for small clusters to flip between different structures of closely similar energy is noted and needs more systematic investigation. Since the crystal or icosahedral structures he observes are rarely perfect, it may seem a little surprising as well as gratifying to the microscopist that they ever show up as magic numbers in larger molecular beam clusters.

To increase the overlap between the two techniques, new experiments are now urgently needed, such as more direct studies of structure in molecular beam equipment and more studies of excitations and electronic structure in the electron microscope. The molecular beam work has opened our eyes to the number-sensitive and key role which electron as well as atomic shell structure can play. Major efforts are therefore required to produce supported samples with arrangements of essentially identical particles. This will very probably involve the use of single-crystal supports with well characterised surface or interior sites, *e.g.* zeolite cages,[74,75] but whether conventional evaporation methods, cluster chemistry techniques or some soft-landing form of molecular beam technology will prove successful in this is not yet clear. At least for surface sites the scanning tunnelling microscope appears to be potentially capable of analysing the results[76] as a valuable supplement to the STEM. Such samples would open up many new and exciting possibilities for less damaging broad beam spectroscopies and structural investigation. For instance, clusters in identical orientation could provide suitable samples for angle-resolved photoelectron spectroscopy or even low-energy electron holography.

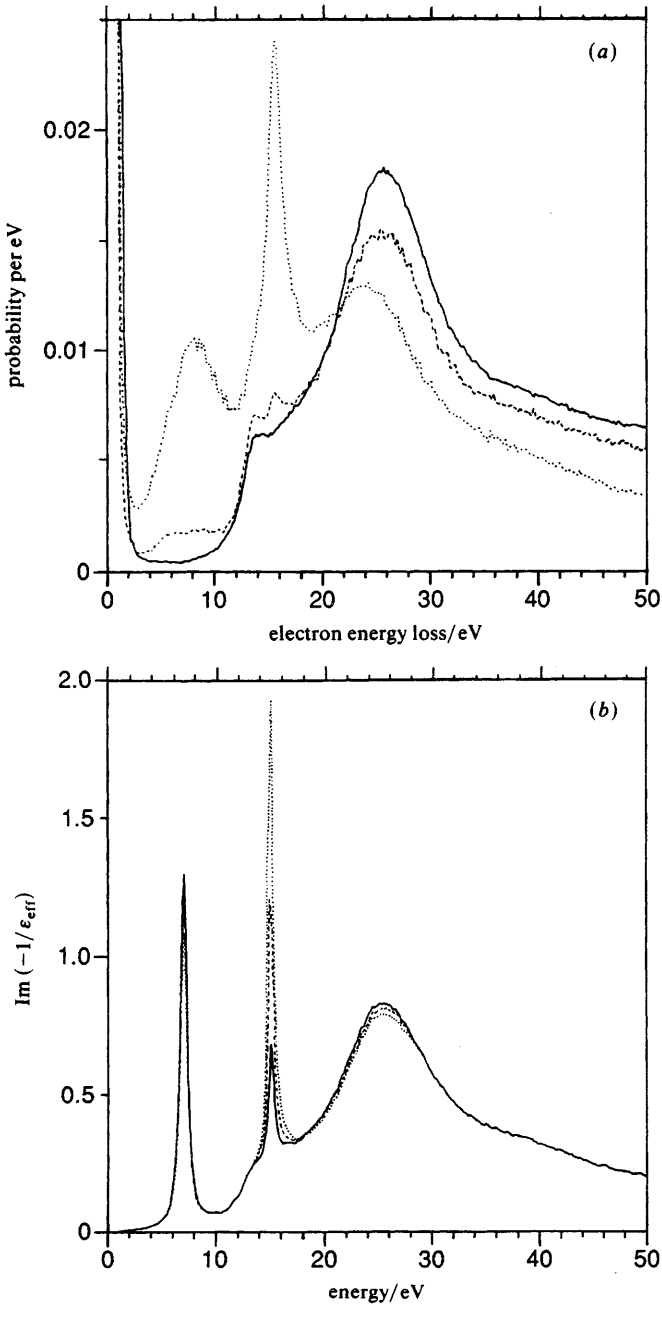


**Fig. 4** (*a*) Electron energy loss spectra observed[70] during the process of electron beam damage of $AlF_3$ leading to the formation of a colloidal dispersion of small Al particles. The development of the interface loss 6–8 eV and the bulk Al plasma loss peak at 15 eV with increasing damage can be seen (full, broken and dotted curves respectively). (*b*) Energy loss function for Al spheres (volume fraction $f = 0.1$) in an $AlF_3$ matrix computed using eqn. (2) for sphere radii $a$ of 0.5, 1.5 and 5 nm (full, broken and dotted curves respectively)

It will also be important to extend the structural computations of small clusters to include the effects of the surroundings and even of molecules reacting at the cluster surface. Whether different faces or sites on small clusters are specially active may be related to possible variations in local work function at different points on the particle and the concomitant external electric fields that such variations would generate. The time must be approaching when more detailed computations will be able to throw additional light on this unresolved question.

As usual, one may expect a strongly non-linear relation between the number of different measurements or related computations which can be made on a given sample and the dividends which result. The scientists from the many different disciplines which are relevant to the exploration of these exciting prospects have thus an added impetus to improve their mutual understanding at meetings such as this.

I am grateful to the SERC, the Wolfson Foundation, B.P. and ICI for supporting our work in electron microscopy in Cambridge. Warm thanks are also due to R. Haydock, R. Godby, R. M. Lambert, D. W. McComb, J. Buglass and C. A. Walsh for helpful discussions and for providing material for figures. Permission from the American Physical Society to reproduce Fig. 1 and 2 and from the Institute of Physics to reproduce Fig. 3 is gratefully acknowledged.

## References

1 M. Faraday, *Philos. Trans. R. Soc. London*, 1857, **147**, 145.
2 W. A. de Heer, W. D. Knight, M. Y. Chou and M. L. Cohen, *Solid State Phys.*, 1987, **40**, 93.
3 M. L. Cohen, M. Y. Chou, W. D. Knight and W. A. de Heer, *J. Phys. Chem.*, 1987, **91**, 3141.
4 S. Bjørnholm, *Contemp. Phys.*, 1990, **31**, 309.
5 T. P. Martin, T. Bergmann, H. Göhlich and T. Lange, *J. Phys. Chem.*, 1991, **95**, 6421.
6 I. Katakuse, T. Ichihara, Y. Fujita, T. Matsuo, T. Sakurai and H. Matsude, *Int. J. Mass Spectrom. Ion Process.*, 1985, **67**, 229.
7 O. Echt, K. Sattler and E. Recknagel, *Phys. Rev. Lett.*, 1981, **47**, 1121.
8 J. Farges, M. F. De Feraudy, B. Raoult and G. Torchet, *J. Chem. Phys.* 1986, **84**, 3491.
9 S. Bjørnholm, J. Borggren, O. Echt, K. Hansen, J. Pedersen and H. D. Rasmussen, *Phys. Rev. Lett.*, 1990, **65**, 1627.
10 H. Göhlich, T. Lange, T. Bergmann and T. P. Martin, *Phys. Rev. Lett.*, 1990, **65**, 748.
11 T. P. Martin, T. Bergmann, H. Göhlich and T. Lange, *Chem. Phys. Lett.*, 1990, **172**, 209.
12 K. Selby, M. Vollmer, J. Masui, V. Kresin, W. A. de Heer and W. D. Knight, *Phys. Rev. B*, 1989, **40**, 5417.
13 C. Brechignac, M. Broyer, Ph. Cahuzac, G. Delacretaz, P. Labostie, J. P. Wolf and L. Woste, *Phys. Rev. Lett.*, 1988, **60**, 275.
14 H. Haberland, H. Kornmeier, H. Langosch, M. Oschwald and G. Tanner, *J. Chem. Soc., Faraday Trans.*, 1990, **86**, 2473.
15 T. P. Martin, T. Bergmann, H. Göhlich and T. Lange, *Chem. Phys. Lett.*, 1991, **176**, 343.
16 K. E. Shriver, J. L. Perrson, E. C. Honea and R. L. Whetten, *Phys. Rev. Lett.*, 1990, **64**, 2539.
17 R. L. Whetten, D. M. Cox, D. J. Trevor and M. Kaldor, *Surf. Sci.*, 1985, **156**, 8.
18 P. Fayet, A. Kaldor and D. M. Cox, *J. Chem. Phys.*, 1990, **92**, 254.
19 A. Kaldor and D. M. Cox, *J. Chem. Soc., Faraday Trans.*, 1990, **86**, 2459.
20 O. Cheshnovsky, K. J. Taylor, J. Conceicao and R. E. Smalley, *Phys. Rev. Lett.*, 1990, **64**, 1785.
21 G. Gantefor, M. Gausa, K.-H. Meiwes-Broer and H. O. Lutz, *J. Chem. Soc., Faraday Trans.*, 1990, **86**, 2483.
22 W. Ekart, *Phys. Rev. B*, 1984, **29**, 1558.
23 J. Friedel, *Phase Transitions*, 1990, **24**, 215.
24 R. O. Jones and O. Gunnarsson, *Rev. Mod. Phys.*, 1989, **61**, 689.
25 R. Car and M. Parrinello, *Phys. Rev. Lett.*, 1985, **55**, 2471.
26 U. Rothlisberger and W. Andreoni, *J. Chem. Phys.*, 1991, **94**, 8129.
27 R. O. Jones, *Phys. Rev. Lett.*, 1991, **67**, 224.
28 J. Bernholc, Jae-Yel Yi and D. J. Sullivan, *Faraday Discuss.*, 1991, **92**, 217.
29 P. Ballone, W. Andreoni, R. Car and M. Parinello, *Phys. Rev. Lett.*, 1988, **60**, 271.
30 E. Kaxiras, *Phys. Rev. Lett.*, 1990, **64**, 551.
31 A. Howie, in *Characterisation of Catalysts*, ed. J. M. Thomas and R. M. Lambert, Wiley, Chichester, 1980, ch. VI pp. 89–104.

32 J. V. Sanders, in *Catalysis: Science and Technology*, ed. J. R. Anderson and M. Boudart, Springer, Berlin, 1985, vol. 7 ch. 2.
33 A. K. Dayte and D. J. Smith, *Catal. Rev.*, 1991, in the press.
34 M. Che and C. O. Bennett, *Adv. Catal.*, 1989, **36**, 55.
35 P. A. Buffat, M. Flueli, R. Spycher, P. Stadelmann and J. P. Borel, *Faraday Discuss.*, 1991, **92**, 173.
36 A. I. Kirkland, D. A. Jefferson, D. Tang and P. P. Edwards, *Proc. R. Soc. London, A*, 1991, **434**, 279.
37 L. D. Marks, *Philos. Mag. A*, 1984, **49**, 81.
38 A. Howie and L. D. Marks, *Philos. Mag. A*, 1984, **49**, 95.
39 L. D. Marks and A. Howie, *Nature (London)*, 1979, **282**, 196.
40 J. M. Thomas, *Pure Appl. Chem.*, 1988, **60**, 1517.
41 G. A. Somorjai, *J. Phys. Chem.*, 1990, **94**, 1013.
42 L. D. Marks and D. J. Smith, *Nature (London)*, 1983, **303**, 316.
43 D. A. Jefferson and P. J. F. Harris, *Nature (London)*, 1988, **332**, 617.
44 L. D. Marks and D. J. Smith, *Surf. Sci.*, 1985, **157**, L367.
45 J.-O. Bovin and D. J. Smith, *Nature (London)*, 1985, **317**, 47.
46 S. Iijima and T. Ichikashi, *Phys. Rev. Lett.*, 1986, **56**, 616.
47 A. Howie, *Nature (London)*, 1986, **320**, 684.
48 P. Williams, *Appl. Phys. Lett.*, 1987, **50**, 1760.
49 A. V. Crewe and J. S. Wall, *Science*, 1970, **168**, 1338.
50 A. V. Crewe, J. P. Langmore and M. S. Isaacson, in *Physical Aspects of Electron Microscopy and Microbeam Analysis*, ed. B. M. Siegel and D. R. Blaman, Wiley, New York, 1975, p. 47.
51 M. M. J. Treacy, A. Howie and C. Wilson, *Philos. Mag.*, 1978, **38**, 569.
52 M. M. J. Treacy and S. B. Rice, *J. Microsc.*, 1989, **156**, 211.
53 D. W. McComb, J. H. Paterson, J. G. Buglass and S. L. Friedman, *EMAG 91 Conf. Proceedings*, Institute of Physics, London, in the press.
54 B. F. G. Johnson, J. Lewis, M. Gallup and M. Martinelli, *Faraday Discuss.*, 1991, **92**, 241.
55 A. V. Crewe, *Chem. Scr.*, 1978, **14**, 17.
56 J. C. J. Bart and G. Vlaic, *Adv. Catal.*, 1987, **35**, 1.
57 M. Pan, J. M. Cowley and I. Y. Chan, *Ultramicroscopy*, 1990, **34**, 93.
58 C. E. Lyman, J. S. Hepburn and H. G. Stenger, *Ultramicroscopy*, 1990, **34**, 73.
59 D. Imeson, *J. Microsc.*, 1987, **147**, 67.
60 G. G. Hembree, F. C. H. Luo and J. A. Venables, in *Proc. 49th EMSA meeting*, ed. G. W. Bailey and E. L. Hall, San Francisco Press, San Francisco, 1991 pp. 464–465.
61 O. L. Krivanek, C. C. Ahn and R. B. Keeney, *Ultramicroscopy*, 1987, **22**, 103.
62 D. McMullan, J. M. Rodenburg, Y. Murooka and A. J. McGibbon, *EMAG-MICRO 89 Conf. Proceedings*, Inst. of Physics, London, 1990, p. 55.
63 C. Colliex, D. Ugarte, Z. L. Wang, M. Gasgnier and V. Paul-Boncour, *Surf. Interface Anal.*, 1988, **12**, 3.
64 C. Colliex, J. L. Maurice and D. Ugarte, *Ultramicroscopy*, 1989, **29**, 31.
65 E. Fermi, *Phys. Rev.*, 1940, **57**, 485.
66 Fan Cheng-Gao, A. Howie, C. A. Walsh and Yuan Jr., *Solid State Phenom.*, 1989, **5**, 15.
67 M. G. Walls and A. Howie, *Ultramicroscopy*, 1989, **28**, 40.
68 D. Ugarte, Doctor of Science Thesis, University of Paris-Sud, 1990.
69 F. Ouyang and M. Isaacson, *Ultramicroscopy*, 1989, **31**, 345.
70 A. Howie and C. A. Walsh, *J. Microsc. Microanal. Microstruct.*, 1991, in the press.
71 P. Echenique, J. Bausells and A. Rivacoba, *Phys. Rev. B*, 1987, **35**, 1521.
72 J. C. Maxwell Garnett, *Philos. Trans. R. Soc.*, 1904, **203**, 385.
73 A. von Felde, J. Fink and W. Ekhardt, *Phys. Rev. Lett.*, 1988, **61**, 2249.
74 M. Pan, J. M. Cowley and I. Y. Chan, *Ultramicroscopy*, 1990, **34**, 93.
75 S. B. Rice, J. Y. Koo, M. M. Disko and M. M. J. Treacy, *Ultramicroscopy*, 1990, **34**, 108.
76 D. D. Chambliss, R. J. Wilson and S. Chiang, *Phys. Rev. Lett.*, 1991, **66**, 1721.
77 W. D. Knight, K. Clemenger, W. A. de Heer, W. A. Saunders, M. Y. Chou and M. L. Cohen, *Phys. Rev. Lett.*, 1984, **52**, 2141.


*Paper* 1/04984D; *Received* 27*th September*, 1991